CrystEngComm

Cite this: *CrystEngComm*, 2012, **14**, 8330–8334

www.rsc.org/crystengcomm

COMMUNICATION

Catalyst-free synthesis of single crystalline ZnO nanonails with ultra-thin caps

Xing Huang,[ac] Lidong Shao,[b] Guang-Wei She,[a] Meng Wang,[ac] Shu Chen[ac] and Xiang-Min Meng*[a]

Received 25th July 2012, Accepted 4th October 2012
DOI: 10.1039/c2ce26197a

Arrays of single-crystalline ZnO nanonails with tapering diameters and ultra-thin caps have been successfully synthesized on a silicon substrate *via* a simple catalyst-free thermal evaporation method. Each of the ZnO nanonails consists a nanowire (stem) on the bottom and an ultra-thin symmetrical hexagonal cap on the top. Structural characterization reveals that the synthesized ZnO nanonail has a wurtzite (WZ) structure with a preferred growth direction of [0001] in the stem and <2$\bar{1}\bar{1}$0> in the cap. Remarkably, the ultra-thin cap shows a diameter-to-thickness ratio of over 20 : 1, which is much higher in magnitude than those reported in previous works. Based on the systematic morphological characterization and structural analysis, a self-catalyzed vapor–liquid–solid (VLS) mechanism followed by a vapor–solid (VS) process is proposed to explain the growth of the nanonails. Optical properties are also investigated with Raman and photoluminescence (PL) techniques, which show good crystal quality of the synthesized nanonails.

1 Introduction

Semiconductor nanostructures with various morphologies, including nanowires,[1] nanorods,[2] nanotubes[3] and nanoribbons,[4] have been extensively studied for their potential applications in functional nanoscale devices owing to their novel optical and electrical properties. Being an important II–VI semiconductor, ZnO nanostructures, with a direct band-gap of 3.37 eV and high electron-hole binding energy of 60 meV, have been used in sensors, lasers, displays, solar cells, field emissions, photocatalysis and piezo-nanogenerators,[5–9] *etc.* It is well known that properties of nanostructures are closely related to their structures, including morphology, dimensionality, and crystal structure, *etc.*[10] For instance, the field emission property of ZnO nanorod arrays depends strongly on the shape of their tips.[11,12] With their unique geometries, ZnO nanonails are expected to be valuable not only for fundamental research but also for their potential applications in sensors, photocatalysis and solar cells.[13–16] Considerable efforts have been devoted to prepare ZnO nanonails through thermal evaporation approaches. However, catalysts or additives such as In, In_2O_3 and graphite powder are generally employed, which may introduce impurities to the final product.[17–19] Besides, growth mechanisms of these nanonails are so far controversial. For example, Lao *et al.* ascribe the longer time to absorb the ZnO_x vapor at the top than the bottom to the formation of the cap.[17] On the other hand, Wei *et al.* believe the formation of cap is resulted from the comparable growth velocities of (0001) and {1$\bar{1}$00} planes during the cooling process.[20] Therefore, a simple catalyst-free technique to synthesize high-quality ZnO nanonails and better understanding of their growth mechanisms are highly desirable.

Herein, we report a facile approach for synthesis of ZnO nanonail arrays without using any catalyst or additive. Ultra-thin caps with a high diameter-to-thickness ratio are obtained homogeneously in nail-like nanostructures. Morphology, phase structure, and crystal structure of the product are systematically studied by means of scanning electron microscopy (SEM), X-ray diffraction (XRD), transmission electron microscopy (TEM) and selected-area electron diffraction (SAED) techniques. A growth mechanism for the hierarchical ZnO nanonail is proposed based on the morphological observation and structural analysis. Finally, Raman and PL properties of these materials are investigated and discussed in detail.

2 Experimental details

Arrays of ZnO nanonails were prepared in a quartz tube housed in a high-temperature furnace. Analytical grade Zn powder loaded in a ceramic boat was placed at the center of the tube. A silicon wafer was placed at about 4 cm downstream from the Zn source. After the tube was sealed and evacuated to a pressure of 0.1 Pa, high-purity argon mixed with 5% hydrogen and air were simultaneously fed into the tube at rates of 35 and 40 sccm respectively. The furnace was then heated up to 600 °C at a rate of 25 °C min^{-1} and maintained at 600 °C for 90 minutes at a pressure of 170 Pa. After the reaction, the tube was naturally cooled down to room temperature. Product material as-deposited on the silicon wafer was characterized with SEM (Hitachi S4300), XRD (Bruker D8 Focus), TEM (JEOL 2100F), Raman (inVia-Reflex) and PL (pulsed Nd:YAG laser, Quanta-Ray INDI Series).

[a]*Key Laboratory of Photochemical Conversion and Optoelectronic Materials, Technical Institute of Physics and Chemistry, Chinese Academy of Sciences, Beijing, 100190, China. E-mail: mengxiangmin@mail.ipc.ac.cn*
[b]*Department of Inorganic Chemistry, Fritz Haber Institute of the Max Planck Society, Faradayweg 4-6, Berlin, 14195, Germany*
[c]*University of Chinese Academy of Sciences, Beijing, 100049, China*

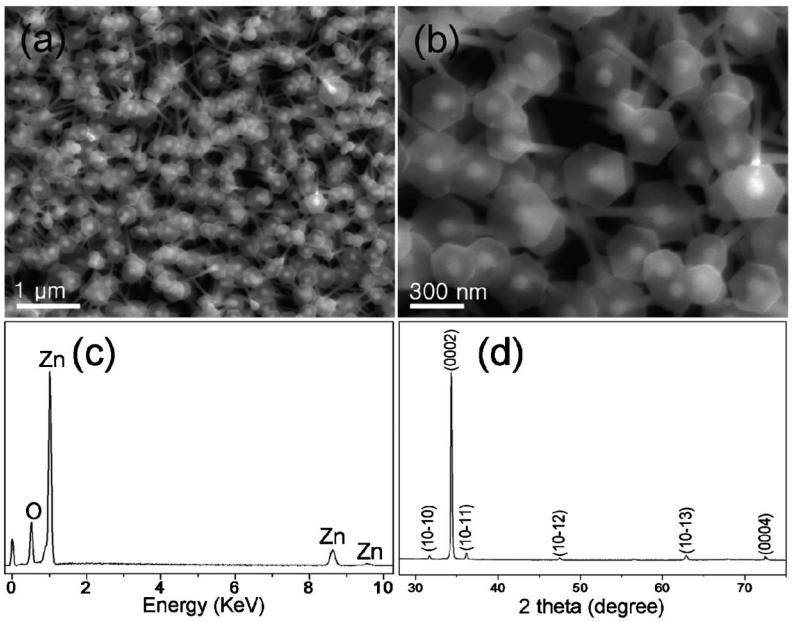

Fig. 1 (a) A low-magnification and (b) enlarged top-view SEM images of the ZnO nanonails with symmetrical hexagonal caps; (c) EDS and (d) XRD spectra of the as-prepared nanonails.

3 Results and discussion

3.1 Morphology and structure

Morphology and composition of the product were characterized with an SEM equipped with energy-dispersive X-ray spectroscopy (EDS) facility. Fig. 1(a) shows a typical top-view SEM image of the synthesized nanostructures which are approximately vertical to the silicon substrate with a length of about 1 μm. An enlarged SEM image in Fig. 1(b) clearly exhibits that each individual nanostructure is comprised of a nanowire on the bottom and a thin symmetrical hexagonal cap on the top, giving a nail-like morphology. The change of diameter from the stem to the cap is abrupt, which implies a rapid change in the growing environment. EDS result indicates that the sample consists of only Zn and O with an atomic ratio of about 1 : 1 (see Fig. 1(c)). Phase composition of the product was analyzed with XRD measurement. As shown in Fig. 1(d), all the diffraction peaks can be indexed to the WZ structured ZnO with lattice constants of a = 0.2498 nm and c = 0.5206 nm (JCPDS, No. 36-1451). The sharp and intense (0002) diffraction peak implies that the as-obtained product is well crystallized in WZ structure with a preferred orientation along the c-axis.

Fig. 2(a) shows a side-view TEM image of a typical ZnO nanonail. The diameter of its stem continually increases from 40 nm at the bottom to about 100 nm at the top. The cap of nail is about 440 nm in diameter and 20 nm in thickness with a high aspect ratio of 22 : 1. To our best knowledge, this is the highest aspect ratio observed in the cap of ZnO nanonails.[17,18,20–22] This feature can be beneficial for applications that require a large surface area.[15] Fig. 2(b) is an enlarged tilted-view TEM image of the same nanonail as shown in Fig. 2(a), which clearly displays a hexagonal shape in the cap. The six side surfaces of the cap are terminated with six equivalent $\{01\bar{1}0\}$ planes due to the intrinsic WZ structure. High-resolution TEM (HRTEM) and SAED studies were carried out to systematically analyze the detailed structure of the ZnO nanonails. As shown in Fig. 2(c), an HRTEM image taken from the stem clearly reveals (0001) and $(01\bar{1}0)$ lattice planes of WZ structured ZnO with an inter-planar spacing of 0.52 and 0.28 nm, respectively. The surface of the stem is clean without showing any amorphous contamination. Fig. 2(d) is the corresponding SAED pattern recorded along the $[2\bar{1}\bar{1}0]$ direction, which confirms a single-crystalline nature and a growth direction of [0001] in the stem of the nanonail. Shown in Fig. 2(e) is a side-view HRTEM image of the cap of a ZnO nanonail. Lattice fringes of WZ type ZnO (0002) planes with d-spacing of 0.26 nm are clearly observed. The corresponding SAED pattern in Fig. 2(f) further demonstrates that the cap is single-crystalline and has preferred growth direction along $<2\bar{1}\bar{1}0>$.

While the majority of the nanonails possess hexagonal shaped caps, nanonails with dodecagonal caps were also observed on the silicon substrate at a different region (Fig. 3(a) and (b)). It was found that the dodecagonal caps are generally larger in diameter than the hexagonal caps. The change of morphology is due to the different local experimental conditions, for example, temperature gradient.[23] Shown in Fig. 3(c) is a top-view TEM image of a dodecagonal cap of a nanonail. The dark area marked with white dashed line in the center is the stem of the nanonail. The hexagonal shape reveals a growth direction along [0001] in the stem. The adjacent planes in the cap shows an angle of 150°, which can be indexed to the $\{01\bar{1}0\}$ and $\{2\bar{1}\bar{1}0\}$ facets based on the WZ crystallographic characteristic of ZnO. We speculate that the comparable growth rate in the $<01\bar{1}0>$ and $<2\bar{1}\bar{1}0>$ directions results in the formation of the dodecagonal caps, as schematically illustrated in Fig. 3(d). It is noteworthy that the area of the $\{2\bar{1}\bar{1}0\}$ facets is smaller than that of the $\{01\bar{1}0\}$ facets (see Fig. 3(c)). This is probably because the appearance of additional $\{2\bar{1}\bar{1}0\}$ facets leads to an increasing of the system energy due to the relative higher surface energy of $\{2\bar{1}\bar{1}0\}$ than $\{01\bar{1}0\}$.[24] Thus a

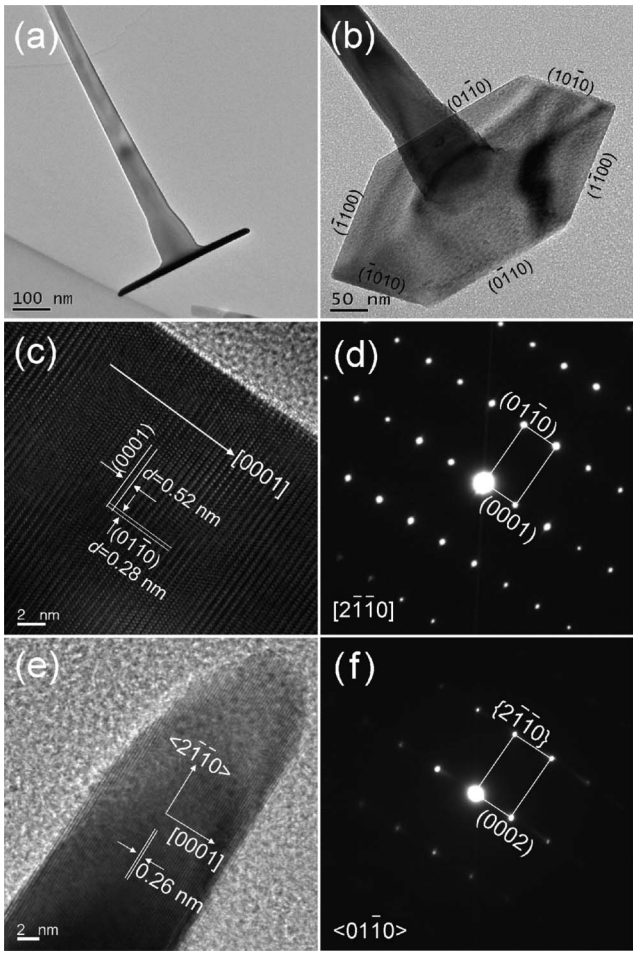

Fig. 2 (a) Side-view and (b) tilted-view TEM images of a typical ZnO nanonail; (c) HRTEM image and (d) corresponding SAED pattern of the nanonail's stem; (e) HRTEM image and (f) SAED pattern of the nanonail's cap.

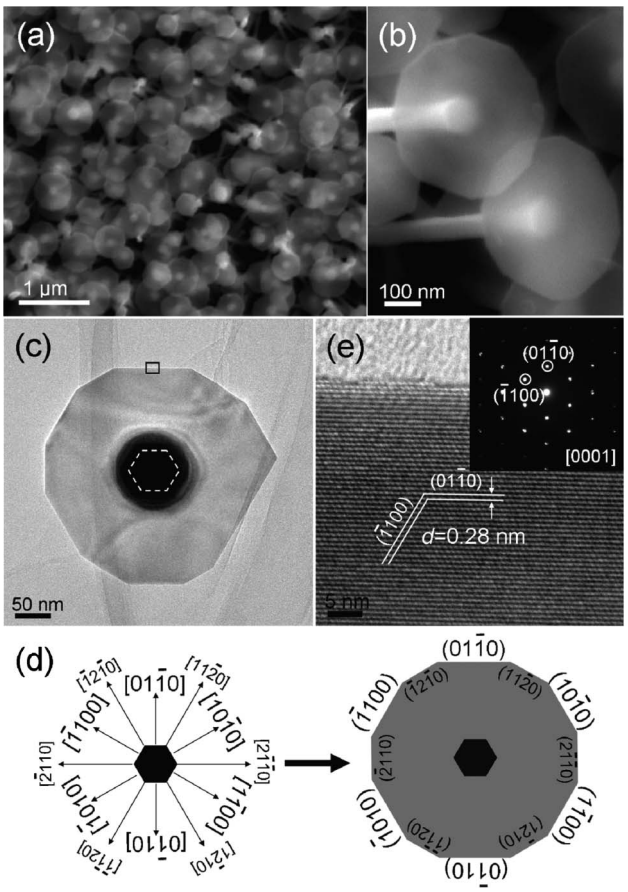

Fig. 3 (a) Low-magnification and (b) enlarged top-view SEM images of ZnO nanonails with dodecagonal caps; (c) top-view TEM image of the cap; (d) schematic model for the formation of dodecagonal cap; (e) HRTEM and corresponding SAED pattern of the cap.

compensation must be made by decreasing the surface area of the {2$\bar{1}\bar{1}$0} facets, which results in a smaller surface area of {2$\bar{1}\bar{1}$0} facets than that of {01$\bar{1}$0}. Fig. 3(e) shows an HRTEM image recorded from the rectangle region in Fig. 3(c). The cap of the nanonail shows a perfect lattice structure, as confirmed by its corresponding SAED pattern (inset of Fig. 3(e)). The *d*-spacing of labeled lattice planes is 0.28 nm which is consistent to {01$\bar{1}$0} planes of WZ type ZnO.

3.2 Growth mechanism

The VLS and the VS processes are two conventional and well-accepted growth mechanisms used for interpreting growth of 1D nanostructures.[25] As a key characteristic in a typical VLS process, a metal nanoparticle (such as gold or silver) catalyst generally appears at the end of the 1D nanostructures. Due to the fact that metal catalysts were not used in our experiment and that no metallic nanoparticles were observed at the tip of nanowires, the conventional VLS mechanism can therefore be ruled out.[5] However, it is important to mention that Zn suboxides (ZnO_x) could also serve as catalysts for the growth of ZnO nanowires based on a so called self-catalyzed and saturated VLS mechanism.[26] With respect to this, the present nanonails may be explained through the following sequences: the growth of basal 1D nanowires assisted with Zn–ZnO_x by a self-catalyzed and saturated VLS mechanism, followed by the formation of 2D hexagonal caps on top of nanowires *via* a VS mechanism. The detailed fabrication process proposed for the growth of nanonails is schematically illustrated in Fig. 4. First, the Zn source was evaporated and reacted with oxygen to form ZnO_x ($x \leqslant 1$) vapor in the quartz tube. The ZnO_x vapor was transported downstream by the carrier gas and then deposited on the silicon substrate to form a ZnO buffer layer. Second, with elevated temperature, the accelerated volatilization rate of the Zn source resulted in a great increase of Zn : O ratio in the vapor, which condensed to form Zn–ZnO_x liquid droplets on the pre-fabricated buffer layer and served as active sites for the subsequent homoepitaxial growth of small ZnO nanowires. With continuous evaporation, oxidization and deposition, arrays of 1D ZnO nanowires with a [0001] growth direction were fabricated *via* the self-catalyzed and saturated process. In the last stage, the volatilization rate of Zn decreased significantly due to the continuous consumption of the source, excessive oxygen would facilitate the formation of ZnO vapor. In such an oxygen-rich condition, the self-catalyzed and saturated process would be hindered due to the lacking supplement of Zn–ZnO_x liquid. Instead, the tips of nanowires would absorb ZnO vapor followed the VS mechanism and start a 2D growth along <2$\bar{1}\bar{1}$0>

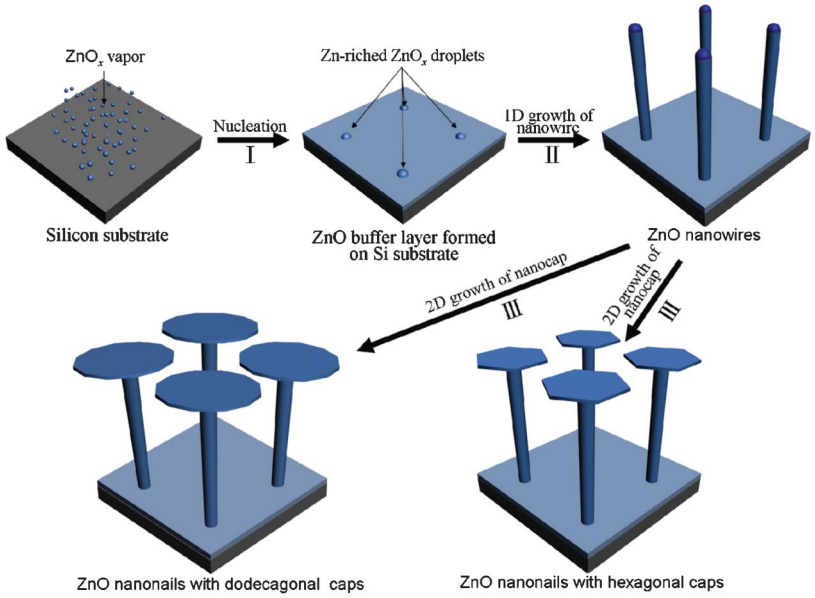

Fig. 4 Schematic illustration for the fabrication process of the synthesized ZnO nanonails.

direction.[13,27] Finally, ZnO nanonails with symmetrical hexagonal caps were formed. The disappearance of Zn-rich ZnO$_x$ droplets on top of nanowires could be ascribed to the continuous consumption and final exhaustion during the lateral growth of the caps.[28] For the nanonail with a dodecagonal cap, as mentioned above, the comparable growth rate in the <01$\bar{1}$0> and <2$\bar{1}\bar{1}$0> directions during the cap growth could be responsible for this. It should be mentioned that formation of hierarchical nanostructures, such as ZnO nanonails, involves quite a complex process. Clearly, additional investigation is required to clarify the detailed growth mechanism of the present nanonails.

3.3 Optical properties

To investigate the optical properties, Raman and PL of the product were performed at room temperature. Shown in Fig. 5(a) is a Raman spectrum of the as-synthesized ZnO nanonails. Several peaks at 331, 377, 437, 574, 657 cm^{-1} can be identified and assigned, respectively, to E_{2H}–E_{2L}, A_{1T}, E_{2H}, A_{1L}, and $3E_{2H}$–E_{2L} of ZnO crystal with WZ phase.[29,30] In particular, the Raman peak at 437 cm^{-1} shows narrower spectral width and much stronger intensity, which demonstrates the good crystal quality of the present nail-like ZnO.[31,32] Fig. 5b is the PL spectrum of the nanonails. A strong near-band-edge (NBE) emission centered at around 385 nm and a relatively low and board deep-level (DL) emission at approximately 505 nm were observed. The UV emission is ascribed to excitonic recombinations at the NBE, while the DL emission is commonly believed to originate from oxygen vacancies.[33] The intense intrinsic emission and weak DL emission imply that the synthesized ZnO nanonails possess high quality crystal structures with fewer structural defects,[32] corresponding well to the Raman result.

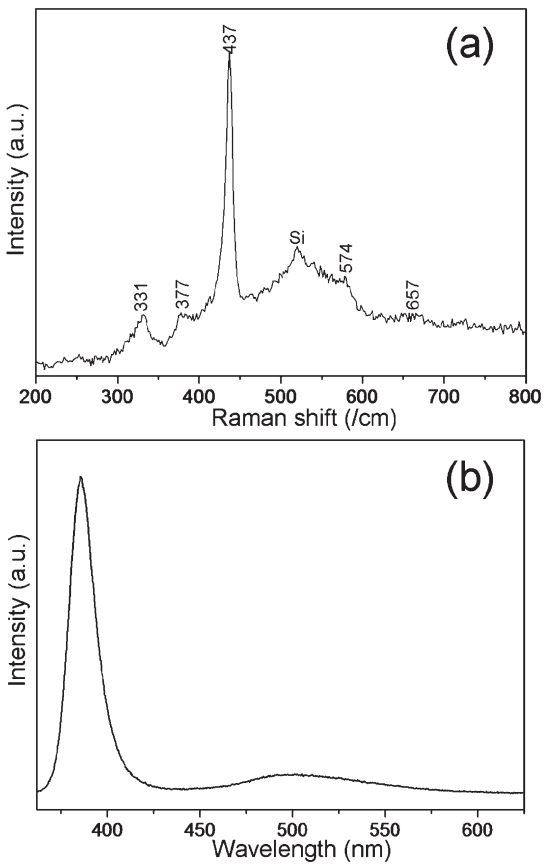

Fig. 5 Room temperature (a) Raman and (b) PL spectra of ZnO nanonails.

4 Conclusions

In summary, arrays of single-crystalline ZnO nanonails with ultra-thin caps have been successfully synthesized through a facile catalyst-free thermal evaporation approach. These nail-like ZnO nanostructures show well-defined morphologies that each nanonail is comprised of a nanowire and a thin symmetrical hexagonal cap. The surface of the nanonail is clean without any amorphous

contamination. Systematic TEM studies reveal that the stem of the nail grows along the [0001] direction, while the cap grows along the $<2\bar{1}\bar{1}0>$ direction. Interestingly, nanonails with dodecagonal caps are also obtained, which may be ascribed to the comparable growth rate of the cap along the $<01\bar{1}0>$ and the $<2\bar{1}\bar{1}0>$ directions. To the best of our knowledge, the obtained diameter to thickness ratio of nanonails' caps is the highest compared with previous reports. The large (0001) surface area has been reported to be useful for improving performance of photocatalysis.[15] The present works may contribute to similar and other applications based on single-crystalline hierarchical ZnO architectures with large nail-caps giving a quasi-two-dimensional morphology. Raman and PL analyses confirm the good crystal quality of the synthesized product. A growth mechanism for the formation of nanonails has been suggested which involves growth of the basal 1D nanowires *via* a self-catalyzed and saturated VLS process, followed by a VS process for the formation of 2D hexagonal caps on top of nanowires. The proposed growth mechanism of ZnO nanonails may give guidance to the rational synthesis of such nanostructures that could be considered for numerous optoelectronic applications.

Acknowledgements

We would like to thank the financial supports from 973 Project (2009CB623003), and the National Natural Science Foundation of China (21073212). We appreciate Dr. E. Kudrenko for valuable discussions.

References

1 Y. Li and Y. Wu, *J. Am. Chem. Soc.*, 2009, **131**, 5851–5857.
2 G. Wang, S. M. Selbach, Y. Yu, X. Zhang, T. Grande and M.-A. Einarsrud, *CrystEngComm*, 2009, **11**, 1958–1963.
3 G. W. She, X. H. Zhang, W. S. Shi, X. Fan, J. C. Chang, C. S. Lee, S. T. Lee and C. H. Liu, *Appl. Phys. Lett.*, 2008, **92**, 053111.
4 Y. Jiang, X. M. Meng, J. Liu, Z. Y. Xie, C. S. Lee and S. T. Lee, *Adv. Mater.*, 2003, **15**, 323–327.
5 G. Z. Shen, Y. Bando, B. D. Liu, D. Golberg and C. J. Lee, *Adv. Funct. Mater.*, 2006, **16**, 410–416.
6 Z. L. Wang, *Chin. Sci. Bull.*, 2009, **54**, 4021–4034.
7 Z. L. Wang, *Mater. Sci. Eng., R*, 2009, **64**, 33–71.
8 Z. L. Wang and J. H. Song, *Science*, 2006, **312**, 242–246.
9 X. Y. Liu, C. X. Shan, S. P. Wang, Z. Z. Zhang and D. Z. Shen, *Nanoscale*, 2012, **4**, 2843–2846.
10 Z. G. Chen, L. N. Cheng, H. Y. Xu, J. Z. Liu, J. Zou, T. Sekiguchi, G. Q. Lu and H. M. Cheng, *Adv. Mater.*, 2010, **22**, 2376–2380.
11 Q. Zhao, H. Z. Zhang, Y. W. Zhu, S. Q. Feng, X. C. Sun, J. Xu and D. P. Yu, *Appl. Phys. Lett.*, 2005, **86**, 203115.
12 R. T. R. Kumar, E. McGlynn, C. McLoughlin, S. Chakrabarti, R. C. Smith, J. D. Carey, J. P. Mosnier and M. O. Henry, *Nanotechnology*, 2007, **18**, 215704.
13 S. Kar, B. N. Pal, S. Chaudhuri and D. Chakravorty, *J. Phys. Chem. B*, 2006, **110**, 4605–4611.
14 A. Umar, M. M. Rahman, S. H. Kim and Y. B. Hahn, *Chem. Commun.*, 2008, 166–168.
15 A. McLaren, T. Valdes-Solis, G. Q. Li and S. C. Tsang, *J. Am. Chem. Soc.*, 2009, **131**, 12540–12541.
16 L. Jinzhang, L. Soonil, Y. H. Ahn, P. Ji-Yong, K. K. Ha and P. K. Ho, *Appl. Phys. Lett.*, 2008, **92**, 263102.
17 J. Y. Lao, J. Y. Huang, D. Z. Wang and Z. F. Ren, *Nano Lett.*, 2003, **3**, 235–238.
18 G. Z. Shen, J. H. Cho and C. J. Lee, *Chem. Phys. Lett.*, 2005, **401**, 414–419.
19 G. Shen, Y. Bando and C. J. Lee, *J. Phys. Chem. B*, 2005, **109**, 10779–10785.
20 O. Y. Wei and Z. Jing, *Mater. Lett.*, 2008, **62**, 2557–2560.
21 M. S. Kumar, D. Chhikara and K. M. K. Srivatsa, *Cryst. Res. Technol.*, 2011, **46**, 991–996.
22 Y. J. Fang, Y. W. Wang, Y. T. Wan, Z. L. Wang and J. A. Sha, *J. Phys. Chem. C*, 2010, **114**, 18022–18022.
23 Z. W. Pan, S. Dai, D. B. Beach and D. H. Lowndes, *Nano Lett.*, 2003, **3**, 1279–1284.
24 B. Meyer and D. Marx, *Phys. Rev. B: Condens. Matter*, 2003, **67**, 035403.
25 Y. F. Hao, G. W. Meng, Z. L. Wang, C. H. Ye and L. D. Zhang, *Nano Lett.*, 2006, **6**, 1650–1655.
26 C. Y. Geng, Y. Jiang, Y. Yao, X. M. Meng, J. A. Zapien, C. S. Lee, Y. Lifshitz and S. T. Lee, *Adv. Funct. Mater.*, 2004, **14**, 589–594.
27 D. H. Fan, R. Zhang and X. H. Wang, *Phys. E.*, 2010, **42**, 2081–2085.
28 Y. G. Yan, L. X. Zhou, Z. D. Han and Y. Zhang, *J. Phys. Chem. C*, 2010, **114**, 3932–3936.
29 Y. J. Xing, Z. H. Xi, Z. Q. Xue, X. D. Zhang, J. H. Song, R. M. Wang, J. Xu, Y. Song, S. L. Zhang and D. P. Yu, *Appl. Phys. Lett.*, 2003, **83**, 1689–1691.
30 K. A. Alim, V. A. Fonoberov, M. Shamsa and A. A. Balandin, *J. Appl. Phys.*, 2005, **97**, 124313.
31 L. Chow, O. Lupan, H. Heinrich and G. Chai, *Appl. Phys. Lett.*, 2009, **94**, 163105.
32 A. Umar, S. H. Kim, Y. S. Lee, K. S. Nahm and Y. B. Hahn, *J. Cryst. Growth*, 2005, **282**, 131–136.
33 Q. Cheng and K. Ostrikov, *CrystEngComm*, 2011, **13**, 3455–3461.

